RESEARCH

Open Access

Check for updates

Optimized administration of human embryonic stem cell-derived immunity-and-matrix regulatory cells for mouse lung injury and fibrosis

Dingyun Song[1,2†] , Zhongwen Li[3,4,5†], Faguo Sun[3,4,6†], Kaiwei Wu[1,10†], Kan Zhang[2], Wenjing Liu[5], Kaidi Liu[2], Bin An[3,4], Zai Wang[8], Tiemei Zhao[2], Huaiyong Chen[2,11,12], Li Xiao[2,13], Liu Wang[3,4,5,6], Lixin Xie[2], Wei Li[3,4,5,6], Liang Peng[9], Jie Hao[3,4,5,6,7*], Jun Wu[3,4,5,6*] and Huaping Dai[1*]

Abstract

Background Lung injury and pulmonary fibrosis (PF), frequently arising as sequelae of severe and acute lung disease, currently face a dearth of effective therapeutic potions. Mesenchymal stem cells (MSCs) with immunomodulatory and tissue repair functions have immense potential to treat lung injury and PF. However, the optimal route of administration, timing, and frequency of dosing remain elusive. Human embryonic stem cell-derived immunity-and-matrix-regulatory cells (IMRCs) have shown therapeutic potential for lung injury and PF.

Methods To ascertain the optimal therapeutic regimen for IMRCs in PF, we conducted an experimental study. Utilizing a mouse model of PF induced by bleomycin (BLM), IMRCs were administered via either a single or double intravenous (IV) or intratracheal (IT) injection on the first and seventh days post-BLM induction.

Results Our findings revealed that IV infusion of IMRCs surpassed IT infusion in enhancing survival rates, facilitating body weight recovery, and optimizing Ashcroft and Szapiel scores among the model mice. Notably, IV administration exhibited a more profound ability to mitigate lung inflammation and fibrosis. Moreover, earlier and more frequent administrations of IMRCs were found to be advantageous in enhancing their therapeutic effects. Specifically, early administration with two IV infusions significantly improved body weight, lung organ coefficient, pulmonary ventilation and diffusion functions, and PF. This was accompanied by an increase in alveolar type I and II epithelial cells and a suppression of macrophage infiltration via CD24.

Conclusion Collectively, these results suggested that IMRCs infusion ameliorated lung injury by promoting lung regeneration and inhibiting macrophage infiltration in a route, time, and frequency-dependent manner.

†Dingyun Song, Zhongwen Li, Faguo Sun and Kaiwei Wu have contributed equally to this work.

*Correspondence:
Jie Hao
haojie@ioz.ac.cn
Jun Wu
wuxf@ioz.ac.cn
Huaping Dai
daihuaping@ccmu.edu.cn
Full list of author information is available at the end of the article

Song *et al. Stem Cell Research & Therapy*   (2024) 15:344

Page 2 of 14

Background

Idiopathic pulmonary fibrosis (IPF) is a chronic and progressive interstitial lung disease with an elusive etiology. IPF predominantly affects middle-aged and elderly individuals, and is characterized by a gradual exacerbation of dyspnea and irreversible deterioration of pulmonary function[1]. Although the discovery and application of antifibrotic drugs pirfenidone and nintedanib have brought hope to IPF patients in the past decade, the disease progression of most patients is still irreversible and disease mortality remains high. The median survival duration for patients who do not undergo lung transplantation is approximately 3 to 5 years following diagnosis [2, 3].

Stem cell therapy represents a promising and burgeoning therapeutic approach for managing a spectrum of degenerative disorders, including IPF. Among these, immunity-and-matrix-regulatory cells (IMRCs), mesenchymal-like stem cells derived from human embryonic stem cells (hESCs), possess several notable advantages such as abundant availability, an absence of teratoma formation, exceptional homogeneity, and the circumvention of tumorigenicity and immune rejection risks [4]. Moreover, IMRCs showed a good therapeutic effect in a mouse model of bleomycin (BLM)-induced lung injury [4], and have been used to treat COVID-19 critical illness (NCT04331613) [5] and PF (ChiCTR2000031139) [6] in patients caused by severe acute respiratory syndrome coronavirus 2 (SARS-CoV-2) infection. However, owing to the limited number of cases, more data are needed to optimize treatment of lung injury and PF with IMRCs. Crucially, the limited preclinical evidence supporting the application of IMRCs in IPF underscores the necessity for prudence in future research endeavors, particularly pertaining to the optimal route of administration, timing, and dosing intervals. Nonetheless, the establishment of standardized protocols could motivate scientists to delve deeper into the therapeutic potential of MSCs for IPF patients.

In this study, the administration of IMRCs transplantation was optimized in mice with BLM-induced lung injury and PF, including the optimal route, timing, and frequency of administration. These results showed that intravenous infusion of IMRCs over intratracheal delivery, highlighting its greater therapeutic potential. Moreover, double intervention at an earlier stage was pivotal in facilitating the treatment of PF. Mechanistically, IMRCs ameliorated lung injury and PF by increasing the population of alveolar type I and type II epithelial cells, while concurrently suppressing macrophage infiltration.

Methods

IMRCs harvesting and culture

IMRCs were prepared as previously described [4, 7]. Briefly, IMRCs were generated by passaging cells that migrated out from human embryoid bodies (hEBs) with serum-free reagents. To generate hEBs, hESCs were dissociated into small clumps and cultured to form hEBs for 5 days. Subsequently, hEBs were transferred onto vitronectin-coated plates and cultured for 14 additional days. During this period, outgrowth from the hEBs occurred. The outgrowth cells were dissociated and passaged in IMRCs medium. After five passages in culture, IMRCs were harvested. These cells displayed a fibroblastic morphology, expressed canonical MSC-specific surface markers (including CD73, CD90, CD105 and CD29), and were negative for typical hematopoietic markers (CD45, CD34, and HLA − DR).

Mice

C57BL/6 J mice were purchased from Beijing Weitonglihua Experimental Animal Technology Co., Ltd. (Beijing, China) and raised in the animal room of China Japan Friendship Institute under specific pathogen-free conditions. The room temperature was maintained at 20–25 °C, with a relative humidity of 40–70%, illumination of 15–20 LX, and 12 h light/dark cycle. Male mice aged 6–8 weeks and weighing about 25 g were selected for preparation of the BLM-induced mouse PF model. The initial body weight of animals varied by no more than 20% of the average body weight. All animals underwent adaptive feeding for a duration of 7 days, during which daily clinical observations were rigorously conducted. Prior to grouping, a comprehensive clinical assessment was performed to ensure accuracy. Only animals meeting the prescribed criteria were advanced to the formal testing phase, while the remaining animals were humanely euthanized with carbon dioxide. Mice were allowed to feed freely. Filtered disinfected drinking water was freely supplied to mice by drinking water bottles. The general conditions of mice were monitored according to institutional guidelines, including their fur condition, activity, and weight. Mice were sacrificed at each observation timepoint by intraperitoneal injection of excess pentobarbital. The animal research committee of China Japan Friendship Hospital (Beijing, China) approved all mouse

studies (No. 190108). Our reporting of animal experiments adheres to the ARRIVE guidelines 2.0.

Cell transplantation in BLM mouse model of pulmonary fibrosis

The mouse was injected intratracheally with 1.5 mg/kg bleomycin sulfate (BLM; Bioway, Xiamen, China; DP721) dissolved in normal saline to generate PF model under anesthesia. IMRCs were delivered intravenously on day 1 or day 7 post-injury. Mice were euthanized with 50 mg/mL sodium pentobarbital (0.6 mg/10 g body weight). Animals were sacrificed 21 days after BLM injection. Following perfusion with normal saline, the left lungs were reserved for morphometric analysis and the right lungs were excised for subsequent analyses.

Histological staining and immunostaining staining analysis

Mouse lung histology was performed as follows. Briefly, the lung was dehydrated, paraffin-embedded, and cut into 4 μm sections before staining with H&E and Masson's trichrome to evaluate inflammation and pathological changes, as well as collagen deposition, respectively. To semi-quantitatively evaluate histopathologic changes, Szapiel scoring was used to quantify alveolitis and the Ashcroft score was used to quantify pulmonary lesions [8]. Immunohistochemical staining was performed using antibodies against α-smooth muscle actin (α-SMA; Servicebio, Wuhan, China; GB13044), fibronectin (FN; Servicebio, GB13091), collagen I (COL-I; Servicebio, GB13091), and green fluorescent protein (GFP; Servicebio, GB13227). Immunofluorescence staining was performed using antibodies against F4/80 (Servicebio, GB11027), HOPX (Proteintech, 11419-1-ap), and SPC (Millipore, Burlington, MA; AB3786). ImageJ software was used to isolate regions of interest in histochemistry or fluorescence images, which were then used to analyze total and relative areas of positive staining. Ashcroft and Szapiel scoring of immunohistochemical staining were performed at $100\times$ magnification using an optical microscope (Olympus, Tokyo, Japan); three areas were randomly selected from each of six sections randomly selected for analysis. Scores were assessed separately by two experimentalists.

Lung function

The lung function was detected by flexiVent FX experimental platform (SCIREQ, Montreal, Canada) according to the manufacturer's instructions. On day 21, mice administered with 3% pentobarbital sodium (40 mg/kg) intraperitoneally were fixed in a supine position within 5–8 min, and endotracheally intubated in the middle of a tracheotomy. The indicators of lung function including inspiratory capacity (IC), respiratory resistance (Rrs), static compliance (Crs), elastic resistance (Ers), Newtonian resistance, tissue damping (G), tissue elasticity (H), and forced vital capacity (FVC) were obtained.

Lung coefficient

The lung tissue was weighed with an electronic balance, and the lung coefficient was calculated according to the formula: lung coefficient = lung mass (g)/body mass (kg).

Establish *CD24* knockout IMRCs cell lines

Firstly, *CD24* knockout hESCs were established using CRISPR-Cas9 technology. The existing differentiation system was used to generate the *CD24* knockout IMRCs (IMRCs-*CD24*$^{-/-}$). To determine the success of *CD24* gene knockout, polymerase chain reaction (PCR) and flow cytometry were performed. *CD24* sgRNA: ATTTGGGGCCAACCCAGAGT.

Statistics

All data are expressed as mean ± SEM. Statistical analysis was performed using GraphPad Prism 7.0 statistical software (San Diego, CA). The statistical significance of multiple groups was compared to each other using Tukey's multiple comparison test ANOVA. A P value of < 0.05 was considered statistically significant.

Results

Intravenously administered IMRCs are more efficacious in treating fibrotic lung injury

To assess the effects of different administration routes of IMRCs on fibrotic lung injury, IMRCs were administered intravenously (i.v.) or intratracheally (i.t.) after BLM challenge (Fig. 1a). Survival curves revealed a statistically significant difference between the BLM group and IMRCs-i.v. group (35.00% vs. 70.00%, P = 0.0233), but not between the BLM group and the IMRCs-i.t. group (35.00% vs. 60.00%, P = 0.1167) (Fig. 1b). A notable recovery in body weight was also observed in the IMRCs-i.v. group (Fig. 1c). Moreover, the IMRCs-i.v. group exhibited the most pronounced improvement in lung morphology (Fig. 1d). Histological examination of the BLM group using H&E and Masson staining revealed diffuse pneumonic lesions characterized by disrupted alveolar architecture, septal thickening, enlarged alveoli, and increased infiltration of inflammatory cells in interstitial and peribronchiolar regions (Fig. 1e, f). The Ashcroft score, a crucial indicator of pulmonary fibrosis severity, was significantly elevated in the BLM (bleomycin) group compared to the control group (7.32 vs. 0.12, P < 0.0001), confirming the successful induction of fibrosis (Fig. 1g). Following IMRCs administration via
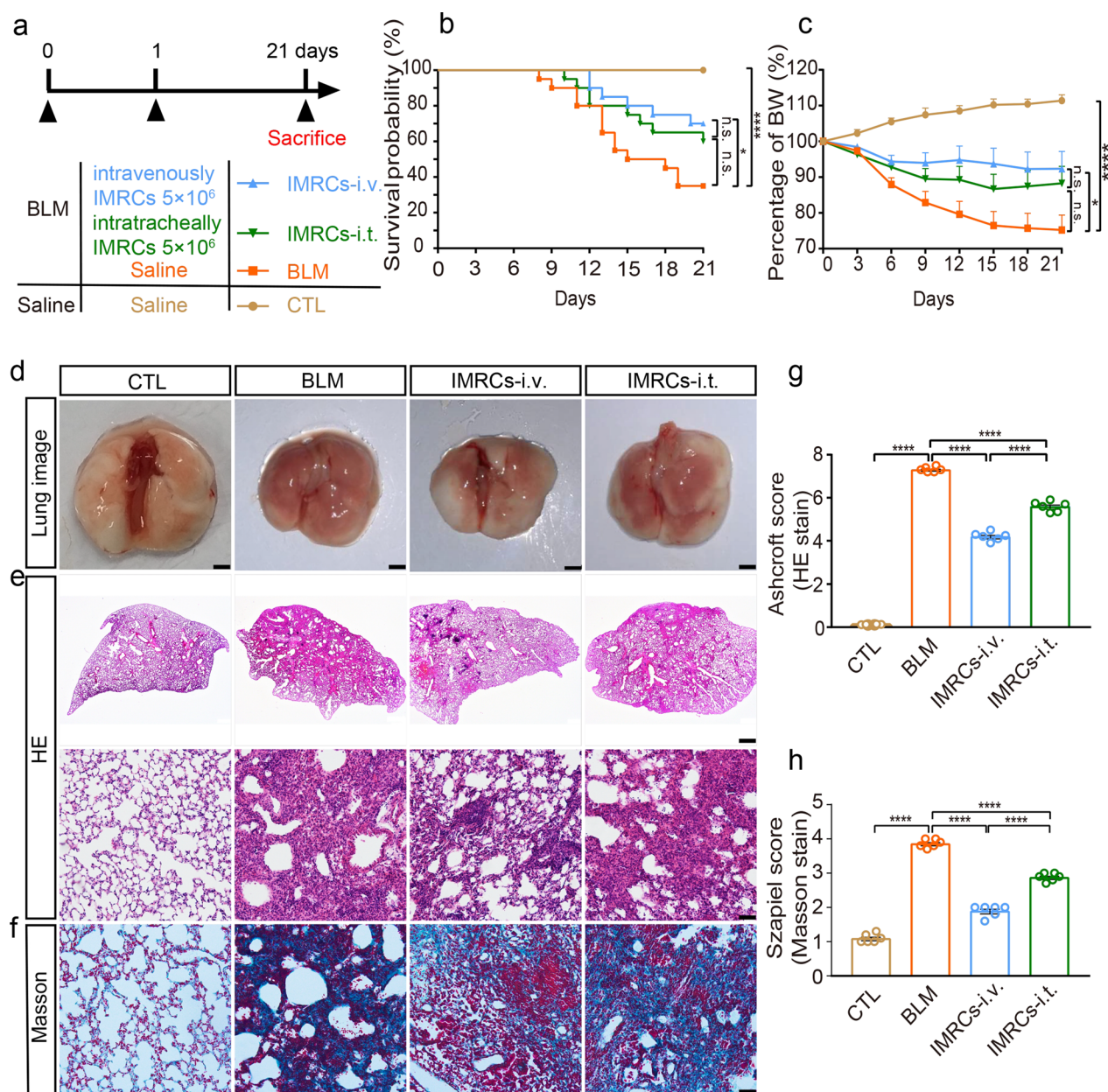
Fig. 1 IMRCs transfusion treats lung injury and fibrosis route dependently. **a** The experimental schema of the in vivo study using different administration routes of IMRCs in mice is shown. Mice were treated with intratracheal bleomycin (BLM; 1.5 mg/kg body weight) or the same amount of saline on day 0. On day 1, some BLM-injured mice received an intravenous (i.v.) or itratracheally (i.t.) injection of 5×10^6 IMRCs via the caudal vein or weasand. A group of BLM-injured mice and normal control mice received the same volume of saline. Mice were randomly grouped (n = 20 per group). **b** Kaplan–Meier survival curves of the mice subjected to different interventions. **c** Relative body weight (%) changes of the mice subjected to different interventions. **d** Representative images of whole lung from all groups on day 21 post-injury. Scale bars, 1.5 mm. **e** Representative histology of lung sections stained with H&E on day 21 post-injury. Scale bars, 500 μm and 50 μm. **f** Representative histology of lung sections stained with Masson's trichrome staining on day 21 post-injury. Scale bars, 50 μm. **g** Evaluation of fibrotic changes by Ashcroft scale in the murine lungs. The Ashcroft scores were measured in the lung H&E section. The severity of fibrotic changes in each section was assessed as the mean score of severity in the observed microscopic fields. Six fields per section were analyzed. **h** Evaluation of fibrotic changes by Szappiel score in the murine lungs. The Szappie scores were measured in the lung Masson's trichrome staining section. The severity of fibrotic changes in each section was assessed as the mean score of severity in the observed microscopic fields. Data was expressed as mean ± SEM. *$P < 0.05$; **$P < 0.01$; ***$P < 0.001$

Song *et al. Stem Cell Research & Therapy*　　　(2024) 15:344

Page 5 of 14

both intravenous and intratracheal routes, a significant reduction in the Ashcroft score was observed in both groups, indicating the therapeutic potential of IMRCs in alleviating fibrosis. The intravenous route of IMRCs administration was significantly more effective in reducing the Ashcroft score compared to the intratracheal route (4.21 vs. 5.60, P < 0.0001) (Fig. 1g). Enhanced collagen deposition in the BLM group contributed to the development of fibrosis, as evidenced by a substantial increase in the Szapiel score following Masson staining (3.87 vs 1.10, P < 0.0001) (Fig. 1h). Conversely, the IMRCs-i.v. group demonstrated a superior ability to alleviate fibrosis compared to the BLM group (1.90 vs 3.87, P < 0.0001), with better-reduced fibrosis compared with the IMRCs-i.t. group (1.90 vs. 2.88, P < 0.0001) (Fig. 1h). These results indicated IMRCs were more effective to treat lung injury through intravenous injection than trachea.

Earlier and double IMRCs administration show better recovery of lung function

To evaluate the optimal infusion time and frequency, IMRCs were administered intravenously in three regimens: a single dose on Day 1 (IMRCs-D1), a single dose on Day 7 (IMRCs-D7), or double doses on both Day 1 and Day 7 (IMRCs-D1&7) (Fig. 2a). Compared to the control group, the BLM group exhibited pronounced lung edema, with a significant increase in edema levels (13.60 vs. 5.54, P < 0.0001) (Fig. 2b). However, both the IMRCs-D1 group and the IMRCs-D1&7 group showed significant alleviation of lung edema, with reductions in the edema levels to 8.41 and 7.76, respectively, compared to the BLM group (Fig. 2b). In contrast, the IMRCs-D7 group failed to show a significant improvement in lung edema (Fig. 2b). Moreover, the IMRCs-D1&7 group exhibited minimal body weight loss (100.60% vs. 75.80%, P = 0.0007), which was comparable to that of the control group (100.60% vs. 108.10%, P = 0.7124) (Fig. 2c). Functionally,

the IMRCs-D1&7 group, which received double IMRCs doses, displayed significant improvements in indices for lung capacity compared with the BLM group, including pressure volume (PV) (0.81 vs. 0.47, P = 0.0015) (Fig. 2d), FVC (1.21 vs. 0.80, P = 0.0080) (Fig. 2e), Crs (0.04 vs. 0.02, P = 0.0042) (Fig. 2f), IC (0.87 vs. 0.56, P = 0.0175) (Fig. 2g), Rrs (0.63 vs. 1.13, P < 0.0001) (Fig. 2h), Ers (21.90 vs. 49.08, P < 0.0001) (Fig. 2i), H (24.37 vs. 46.19, P = 0.0224) (Fig. 2j), and G (4.52 vs. 10.43, P = 0.0005) (Fig. 2k). Importantly, earlier IMRCs administration on day 1 showed superior recovery of lung function compared to later IMRCs administration on day 7 (Fig. 2d-k). These results indicated that IMRCs were more conducive to restore respiratory function by earlier and double intravenous injections.

IMRCs infusion improve pathological changes of fibrotic lung injury

IMRCs infusion improved lung morphology, decreased extracellular matrix deposition including collagen-1 (COL-1), fibronectin (FN) and down-regulated the fibrotic marker expression. Notably, alveolar thickening was more pronounced in mice receiving IMRCs on Day 1 compared to those receiving IMRCs on Day 7 (Fig. 3a). Additionally, IMRCs transplantation positively impacted Ashcroft scores for pulmonary fibrosis (PF), with mice receiving IMRCs on Day 1 exhibiting lower scores than those receiving IMRCs on Day 7, corroborating the previously described results (Fig. 3c). In particular, extracellular matrix deposition (including COL-I, FN, and α-SMA) in mice treated with IMRCs on day 1 was lower compared to those treated on day 7 (Fig. 3b, 3e–3g).

The dual IMRCs infusion protocol was proved to be the most potent in alleviating BLM-induced lung injury, as assessed through parameters such as lung morphology and fibrosis (Fig. 3). Furthermore, the mice received double IMRCs administration exhibited

(See figure on next page.)

Fig. 2 IMRCs transfusion treats lung injury and fibrosis time point- and frequency-dependently. **a** Diagram of the animal experimental protocol for different time and frequency escalation. Mice were treated with intratracheal BLM (1.5 mg/kg body weight) or the same amount of saline on day 0. On day 1, some BLM injured mice received an intravenous injection of 5×10^6, 5×10^6 or saline; and on day 7, the mice which received an intravenous injection of 5×10^6 on day 1 received 2.5×10^6 or saline, the mice which received an intravenous injection of saline on day 1 received 5×10^6. IMRCs via the caudal vein. A group of BLM-injured mice and normal control mice received the same volume of saline. Mice were randomly grouped (n = 15 per group). **b** Lung coefficient (wet lung weight/total body weight) of all treatment groups. **c** Relative body weight (%) changes of the mice subjected to different interventions. **d–k** Lung mechanical function was measured by FlexiVent on day 21, showing PV curves, FVC, Crs, IC, Rrs, Ers, H and G of all the experimental groups. PV, pressure–volume; FVC, forced vital capacity; Crs, static compliance; IC, inspiratory capacity; Rrs, respiratory resistance; Ers, elastic resistance; H, tissue elasticity; G, tissue damping. Data was represented as the mean ± SEM. *P < 0.05; **P < 0.01; ***P < 0.001
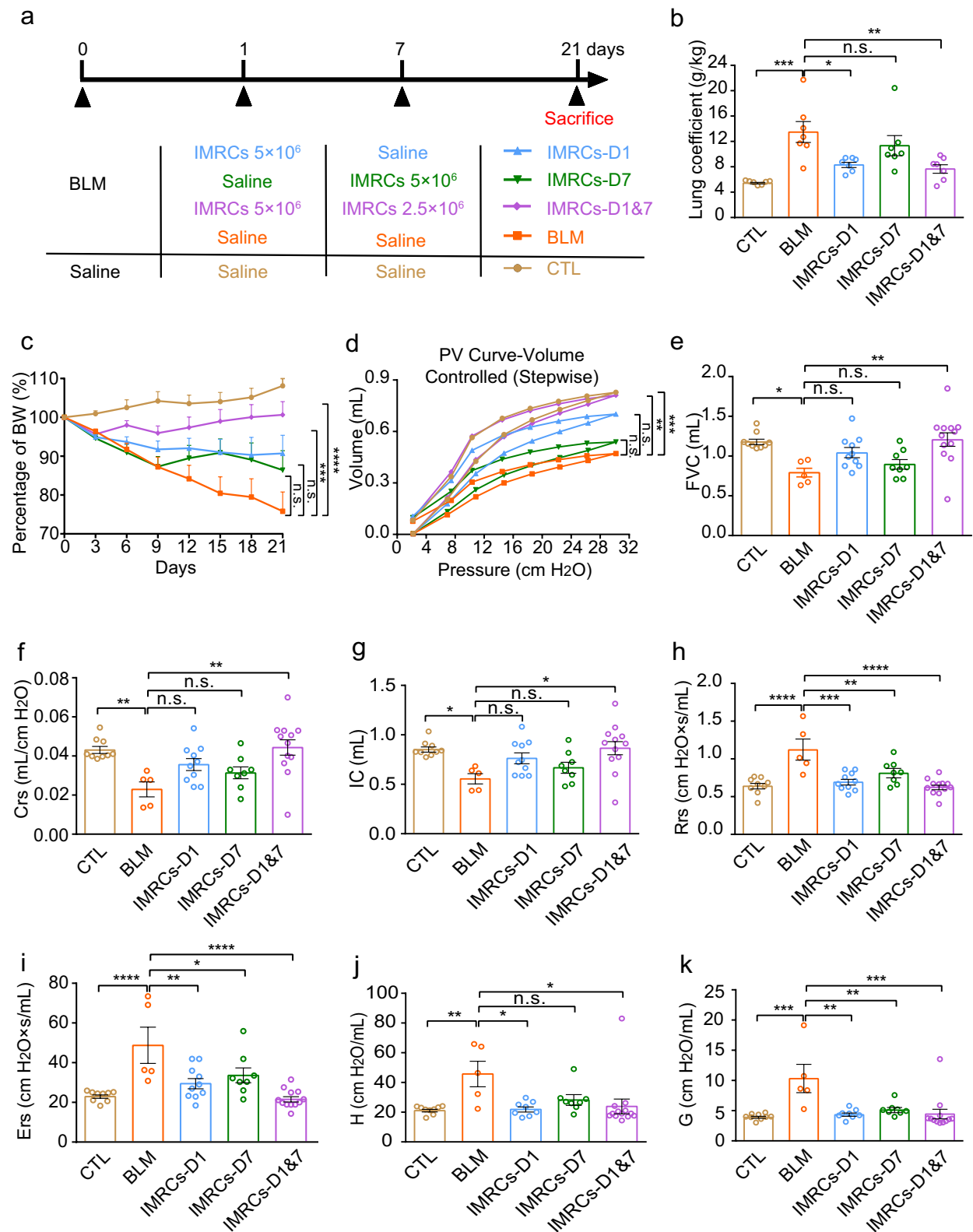
Song *et al. Stem Cell Research & Therapy*   (2024) 15:344

Page 6 of 14

Fig. 2 (See legend on previous page.)

Song *et al. Stem Cell Research & Therapy*   (2024) 15:344

Page 7 of 14

significant improvements in Ashcroft scores and reduced extracellular matrix deposition (Fig. 3).

IMRCs ameliorate fibrotic lung injury by enhancing the ability of self-repairing and immunoregulation

The expression levels of HOPX and SPC in mice treated with IMRCs were significantly elevated compared to those administered BLM alone (Fig. 4a–d), suggesting that IMRCs infusion promoted the regeneration of lung stem cells. In addition, this therapeutic effect occurred in an administration route, time, and frequency-dependent manner. Furthermore, mice infused with IMRCs exhibited significantly reduced F4/80 expression levels compared to BLM-alone controls (Fig. 5a, b), indicating that IMRCs infusion effectively suppressed macrophage infiltration at the site of lung injury. Similarly, IMRCs infusion regulated macrophages and inflammation in an administration route, time, and frequency-dependent manner. Collectively, these results suggested that IMRCs infusion improved lung injury by promoting lung regeneration and inhibiting macrophage infiltration in a route, time, and frequency-dependent manner.

Interestingly, our scRNA-seq results indicated that more than 70% of IMRCs expressed *CD24* compared with primary UCMSCs (< 1%) (Supplementary information, Fig. S1a). Similarly, gene expression analysis by qPCR showed that IMRCs express much higher levels of *CD24* than UCMSCs (Supplementary information, Fig. S1b). It is reported that CD24 plays an important role in regulation of macrophage state[9]. To elucidate the functional role of CD24 in wild type IMRCs (IMRCs-WT), *CD24* knockout IMRCs (IMRCs-$CD24^{-/-}$) was generated by CRISPR-Cas9 system. Firstly, CRISPR-Cas9-*CD24*-sgRNA plasmid was transduced into hESCs to establish hESCs-$CD24^{-/-}$ cell lines. Subsequently, the positive clones were differentiated to IMRCs-$CD24^{-/-}$ as described previously [10]. Sequencing analysis revealed a significant 5-base deletion in exon 1 of IMRCs-$CD24^{-/-}$ compared to wild-type IMRCs (Supplementary information, Fig. S1c). Next, we analyzed the characteristics of IMRCs-$CD24^{-/-}$. Both IMRCs and IMRCs-$CD24^{-/-}$ displayed

similar cell morphology and proliferation rates (Supplementary information, Fig. S1d, e). Flow cytometry analysis further confirmed IMRCs-$CD24^{-/-}$ retained the same surface marker profile as IMRCs, positive for CD105, CD90, CD73, CD29 and HLA-ABC, and negative for CD45, CD34, HLA-DR (Supplementary information, Fig. S1f). Moreover, IMRCs-$CD24^{-/-}$ was negative for expression of CD24 (Supplementary information, Fig. S1f). Subsequent analysis of MSC-specific gene expression patterns showed that IMRCs-$CD24^{-/-}$ exhibited a similar pattern to IMRCs, but distinct from hESCs (Supplementary information, Fig. S1g). To further investigate the immunomodulatory potential, IMRCs and IMRCs-$CD24^{-/-}$ was exposed to the 100 ng/mL pro-inflammatory cytokine IFN-γ for 24 h. After stimulation with IFN-γ, both IMRCs and IMRCs-$CD24^{-/-}$ displayed similar upregulated expression of *IDO1* and *PDL1* (Supplementary information, Fig. S2a, b). When M1 type macrophages were cultured with IMRCs-WT conditioned medium, decreased CD80 protein expression was observed by flow cytometry (76.41% vs 38.96%; Supplementary information, Fig. S2c). However, after *CD24* knockout, the inhibitory effect of IMRCs on M1 macrophages was weakened (38.96% vs 48.65%; Supplementary information, Fig. S2c). These results showed that *CD24* knockout did not affect the basic characteristics of IMRCs, but weakened their regulatory effect on macrophages.

To assess the therapeutic efficacy of IMRCs-$CD24^{-/-}$ on lung fibrosis, IMRCs-$CD24^{-/-}$ were administered intravenously into BLM-induced lung injury mice. The results showed that both the IMRCs-WT and IMRCs-$CD24^{-/-}$ groups significantly improved weight loss in fibrotic mice and reduced the degree of pulmonary fibrosis caused by bleomycin, while the IMRCs-WT group showed more significant weight loss and fibrosis improvement (Fig. 6). These results suggested that CD24 might play an important role in the regulation of macrophages by IMRCs.

Collectively, administering IMRCs in earlier stage, with increased frequency, and via the intravenous route had superior outcomes in ameliorating lung injury, as

(See figure on next page.)

Fig. 3 IMRCs transfusion treats lung injury and fibrosis time point- and frequency-dependently. **a** Representative histology of lung sections stained with H&E and Masson's trichrome on day 21 post-injury. Scale bars, 100 μm. **b** Immunohistochemistry staining (brown) for the protein expression of Collagen-I (COL-I), Fibronectin (FN) and α-smooth muscle actin (α-SMA) in mice subjected to different interventions. Scale bars, 50 μm. **c** Evaluation of fibrotic changes by Ashcroft scale in the murine lungs. The Ashcroft scores were measured in the lung H&E section. The severity of fibrotic changes in each section was assessed as the mean score of severity in the observed microscopic fields. Six fields per section were analyzed. **d** Evaluation of fibrotic changes by Szappiel score in the murine lungs. The Szappie scores were measured in the lung Masson's trichrome staining section. The severity of fibrotic changes in each section was assessed as the mean score of severity in the observed microscopic fields. **e–g** Quantification of the immunohistochemistry staining for Collagen-I **e**, Fibronectin **f**, and α-SMA **g**. Data was expressed as mean ± SEM. *$P < 0.05$; **$P < 0.01$; ***$P < 0.001$
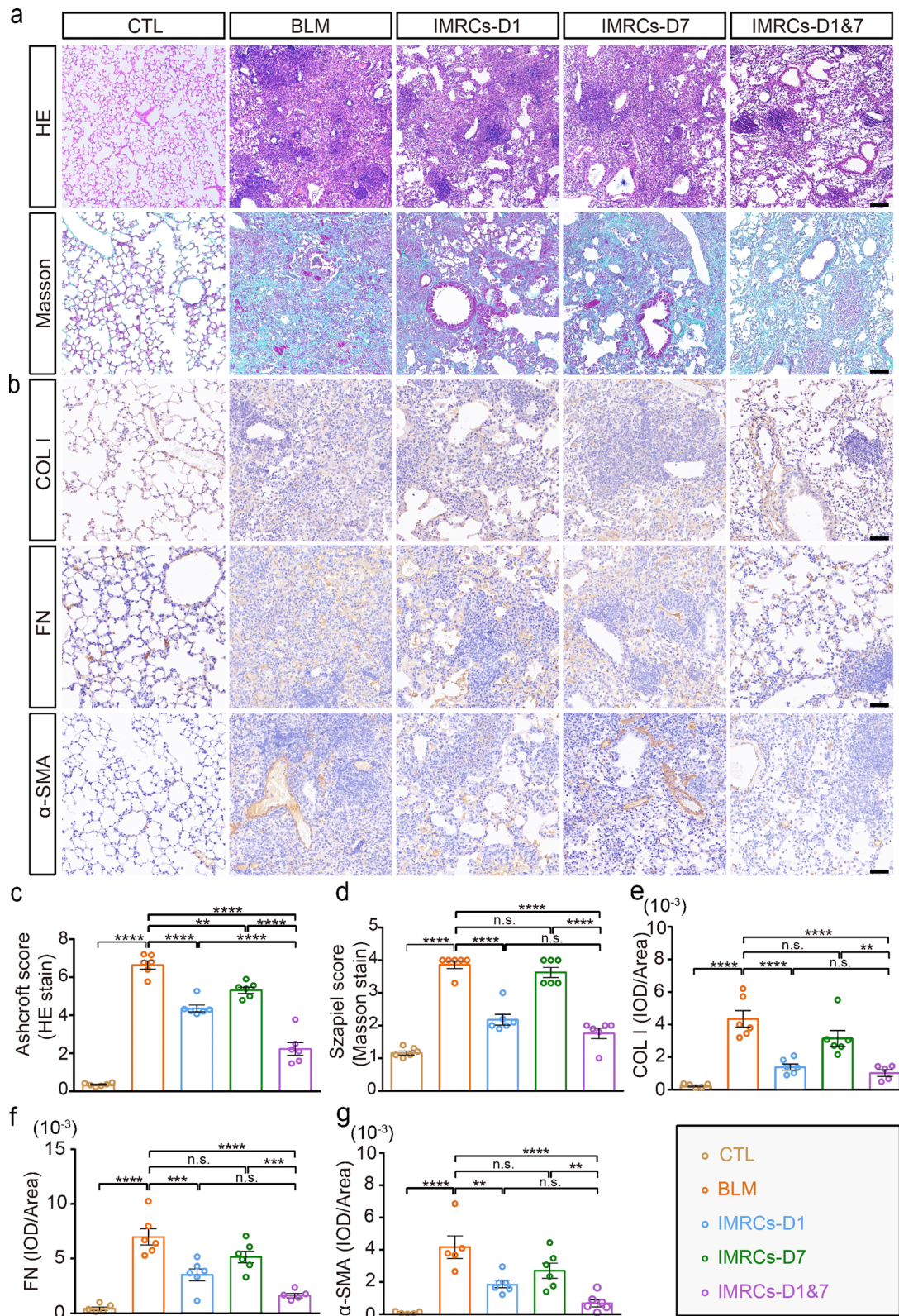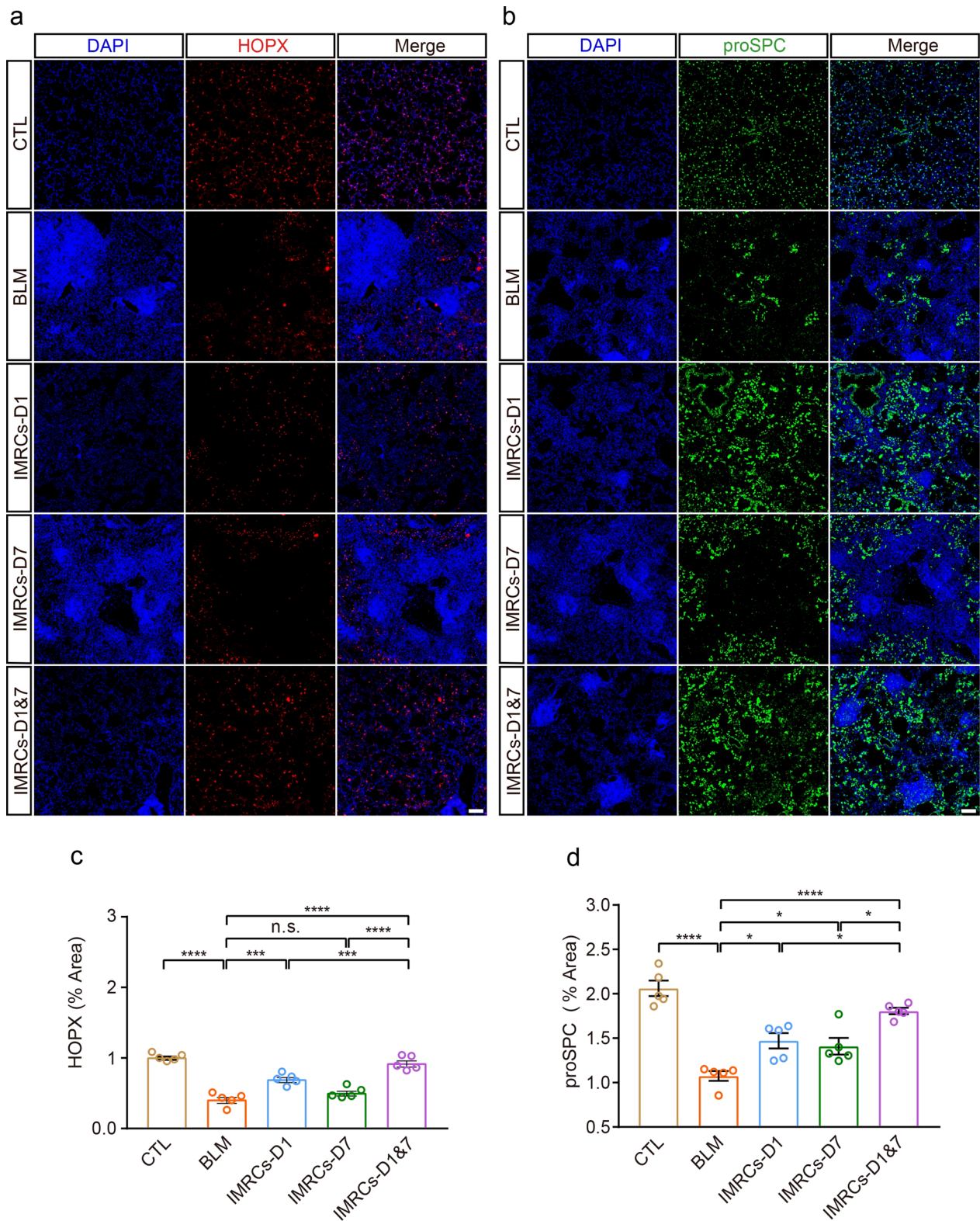
Fig. 3 (See legend on previous page.)

Fig. 4 IMRCs transfusion treats lung injury and fibrosis by promoting regeneration of lung tissue. **a** Immunofluorescent staining (red) for the protein expression of HOPX in mice subjected to different interventions. Scale bars, 100 μm. **b** Immunofluorescent staining (green) for the protein expression of proSPC in mice subjected to different interventions. Scale bars, 100 μm. **c** Evaluation of alveolar type I cells (AT I) by HOPX area in the murine lungs. **d** Evaluation of alveolar type II cells (AT II) by proSPC area in the murine lungs. Data was expressed as mean ± SEM. *$P < 0.05$; **$P < 0.01$; ***$P < 0.001$

Song *et al. Stem Cell Research & Therapy*   (2024) 15:344
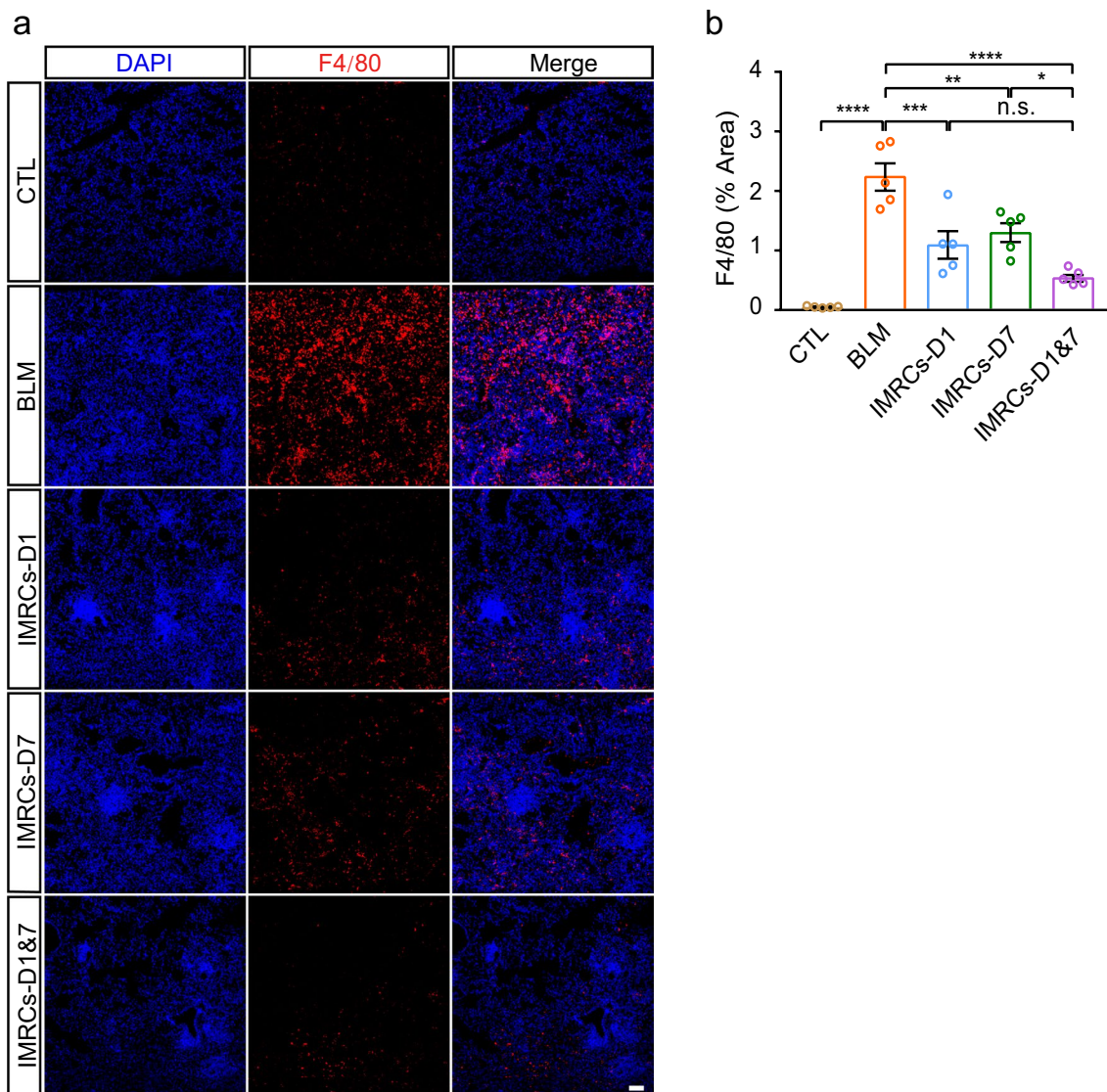
Page 10 of 14

Fig. 5 IMRCs transfusion treats lung injury and fibrosis by inhibiting macrophages infiltration. **a** Immunofluorescent staining (red) for the protein expression of F4/80 in mice subjected to different interventions. Scale bars, 100 μm. **b** Evaluation of macrophage by F4/80 area in the murine lungs. Data was expressed as mean ± SEM. *, $P < 0.05$; **, $P < 0.01$; ***, $P < 0.001$

indicated by inhibition of extracellular matrix deposition and inflammation, and promotion of alveolar epithelial cell proliferation.

Discussion

To optimize the therapeutic efficacy of IMRCs, it is crucial to meticulously consider the delivery route, the number of cells, and the administration schedule (encompassing both single and repeated doses). In our previous study, intravenous administration of IMRCs improved the survival rate of mice in a BLM-induced model (in which diffuse lung lesions develop in a dose-dependent manner following accumulation of BLM in the lung interstitium) by inhibiting both pulmonary inflammation and fibrosis [4]. Specifically, IMRCs inhibited the production of pro-inflammatory cytokines and pro-fibrosis cytokines (such as tumor necrosis factor α and transforming growth factor β1) in lung tissue, while simultaneously safeguarding alveolar type II cells and endothelial cells from damage.

In this study, IMRCs were administered by intratracheal or intravenous injection to evaluate their anti-fibrotic effects against BLM-induced PF. Notably, intravenous administration of IMRCs post-BLM treatment exhibited a more pronounced inhibitory effect. While the underlying mechanisms remain elusive, it is plausible that
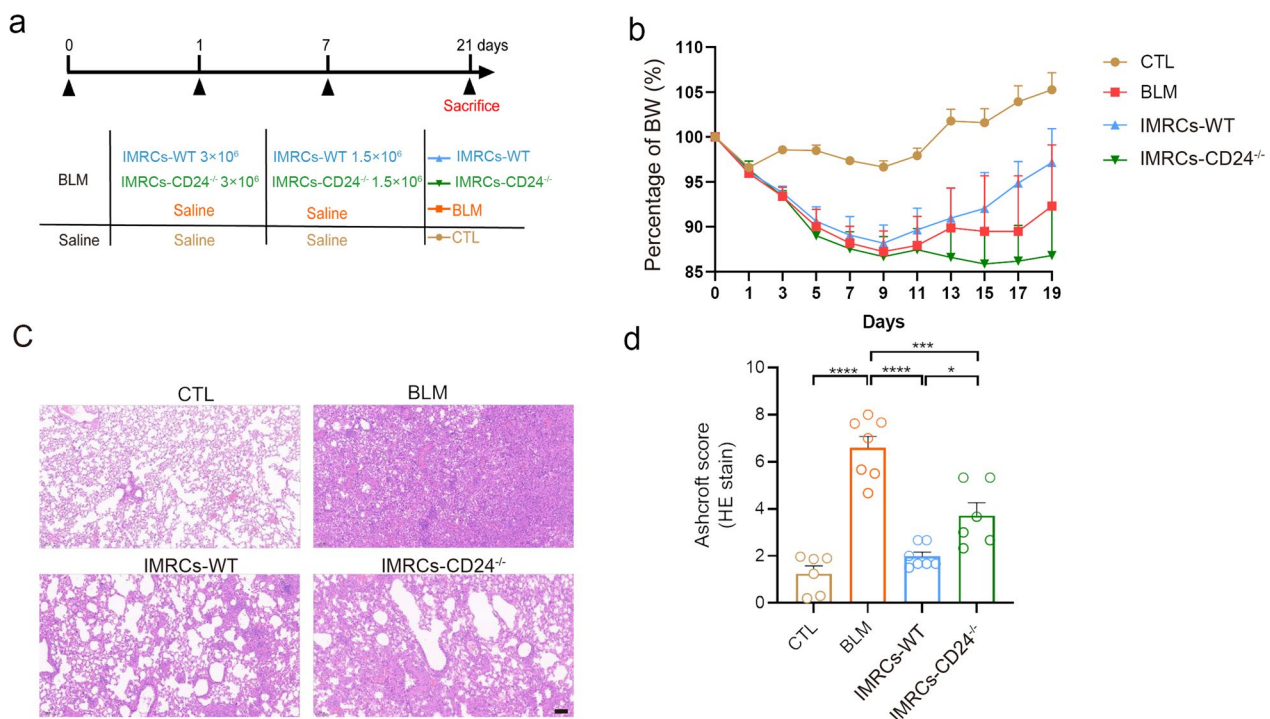
Fig. 6 Knockout of *CD24* reduces the efficacy of IMRCs in treating lung injury and fibrosis. **a** Schematic diagram of animal experiment plan. **b** Weight and mortality statistics of different groups of mice. **c** Representative histology of lung sections stained with H&E. Scale bar, 200 μm. **d** Evaluate the fibrosis changes in the lungs of mice using the Ashcroft scale. The Ashcroft score was measured in the H&E section of the lungs. The data was represented as mean ± SEM. *$P < 0.05$; **$P < 0.01$; ***$P < 0.001$

BLM toxicity may have compromised the functionality of IMRCs when administered concurrently with BLM in this model. Intravenous infusion, a preferred delivery method for therapeutics due to its minimal invasiveness and ease of use, is widely employed for MSC delivery in various lung disorders [11]. Given these advantages, systemic intravenous transplantation emerges as a promising administration route for potential clinical applications in the future.

The administration of MSCs during the inflammatory phase of PF may be hindered by the hostile inflammatory cytokine milieu present in the affected lung tissue. Thus, although higher therapeutic efficacy may be obtained by administering MSCs at an early stage of disease [12], further investigation is necessary for clinical application. Early efficacy of MSCs may be related to the immunomodulatory ability of these cells, which can reduce inflammation and preserve lung epithelium and endothelium, thereby ameliorating lung fibrosis. Conversely, cells transplanted after a delay may not affect collagen deposition or fibrosis progression and may even evoke adverse effects. An alternative approach is a second dose during the developmental phase of PF. In ventilator-induced lung injury, intravenous administration of 2×10^6 bone marrow-derived MSCs (BMSCs) followed by a second

dose was safe and effective for enhancement of lung repair without adverse effects [13]. However, the optimal timing for repeated cell administration needs to be established. Near-infrare fluorescence (NIRF) imaging showed that the cell membrane dark red fluorescent probe fluorescence intensity declined half dramatically by day 6 [4], suggesting a potential window for a second dose. Other researchers found that BMSCs may reach their therapeutic peak and produce soluble factors to ameliorate pulmonary fibrosis 2–3 days after administration [14]. Based on these findings, a second dose of IMRCs was administered 6 days later (7 days after BLM instillation). Our results showed that IMRCs infusion (5×10^6 cells/mouse on day 1 and 2.5×10^6 cells/mouse on day 7) significantly reduced the extent of fibrosis in histological analyses. Furthermore, lung function parameters such as PV curves, IC, Rrs, Crs, Ers, Rn, G, H, and FVC were improved following IMRCs transplantation compared with those in the BLM group. These findings indicated that administration of 5×10^6 cells/mouse at day 1 and 2.5×10^6 cells/mouse at day 7 was the optimal dose and timing.

Injury to alveolar epithelial cells contributes to the pathogenesis of BLM-induced PF [15, 16]. Thus, strategies that promote the proliferation or replenishment of

Song *et al. Stem Cell Research & Therapy*   (2024) 15:344

Page 12 of 14

damaged alveolar epithelial cells may inhibit PF. Previous studies demonstrated that BMSCs adopt the morphological and molecular phenotypes of alveolar type I or II cells to repair damaged lung and reduce PF [17, 18]. However, these phenotypes were not observed in our study. Our in vivo findings reveal that IMRCs localize to the lungs but exhibit a transient presence, completely disappearing after 32 days in mice [4]. Furthermore, only a few IMRCs adopted specific alveolar epithelial phenotypes. These findings were consistent with previous studies [19, 20]. These observations suggested that differentiation might not be the major mechanism for IMRCs-mediated tissue repair. Indeed, the concept of IMRCs engraftment and differentiation is doubtful not only for lung diseases, but also other diseases. In a previous study, high concentrations of hepatocyte growth factor, keratinocyte growth factor, and bone morphogenetic protein-7 were observed in the medium from the silica plus BMSCs group [19]. All these components play crucial roles by accelerating alveolar epithelial cell proliferation and reversing the process of lung fibrosis. Consistent with this, quite a few studies have indicated that the beneficial effects of IMRCs may be related to paracrine mechanisms. Conditioned media from IMRCs contains various soluble factors capable of exerting powerful cytoprotective, anti-inflammatory, and anti-fibrotic effects [4]. IMRCs-derived extracellular vesicles administrated via IT or IV routes were both effective for the treatment of bleomycin-induced pulmonary fibrosis [20]. In our current study, IMRCs facilitated the repair of adjacent alveolar epithelium and inhibited fibrotic processes. Lung histological analyses, including assessments of cellular nodules, alveolar interstitial thickening, and collagen deposition, indicated improvements in the IMRCs group compared to the BLM group. Correspondingly, expression of COL-I, FN, and α-SMA was downregulated. Expression of alveolar epithelial markers (HOPX and SPC) was significantly upregulated in lung tissues where IMRCs focused. In a previous study, conditioned media from BMSCs protected damaged epithelial cells and attenuated BLM-induced pulmonary fibrosis [20]. Taken together, the available in vivo and in vitro data converge to suggest that the protective effects of IMRCs are not attributable to their differentiation into lung cell phenotypes, but instead rely on paracrine mechanisms through released factors to alleviate the lung injury induced by BLM.

Evidence underscores a profound connection between macrophage regulation and CD24 molecules, which are also recognized by the names heat-stable antigen and small cell lung cancer cluster 4 antigen. This highly glycosylated, glycosylphosphatidylinositol-anchored surface protein functions as a pivotal "don't eat me" signal, facilitating cancer cells' evasion of immune surveillance. In 2019, Barkal et.al. reported that CD24 expressed in tumors interacts with the inhibitory receptor sialic acid binding Ig-like lectin 10 (Siglec-10) of macrophages, causing rearrangement of the cytoskeleton of macrophages, thereby blocking Toll-like receptor (TLR) mediated inflammation and cellular phagocytosis, leading to immune escape [9]. CD24 can inhibit the k-light chain enhancement (NF-kB) pathway and cytokine/chemokine production of nuclear factor activated B cells. CD24 can also interact with Siglec-10, inhibiting the destructive inflammatory response of macrophages to infection [21], sepsis [22], liver injury [23], and chronic graft versus host disease. Recently, researchers carried out the Phase I clinical trial (NCT04747574) for the treatment of novel coronavirus infection by preparing CD24 positive exosomes (EXO-CD24). After treatment with EXO-CD24, the inflammatory storm was suppressed, and 29 out of 30 patients were discharged. The above indicates that CD24 plays an important role in the regulation process of macrophages.

This study is subject to several limitations that warrant consideration. Firstly, despite the phenotypic similarities between the mouse BLM model and the acute inflammatory phase of human ARDS, the reproduction of human IPF in our model is incomplete, as evidenced by the diminished observation of fibroblastic foci, alveolar epithelial type II cell hyperplasia, and honeycombing lesions compared to human cases. Notably, the BLM-induced model progresses from an early inflammatory phase to fibrosis after 5–7 days, necessitating an intervention strategy that does not inadvertently suppress fibrosis by merely inhibiting the initial inflammatory response [24]. The early transplantation of IMRCs also faces great difficulties in practical applications. In clinical practice, PF cannot be diagnosed until the disease has progressed to a certain stage. Therefore, further study of IMRCs transplantation in the later stages of BLM-induced pulmonary fibrosis is essential to determine whether IMRCs are effective in eliminating deposited fibrosis. In the future, non-human primate pulmonary fibrosis models may be one of the best options to investigate the underlying mechanisms. In this study, IMRCs were administered at 1 and 7 days after initiation of BLM, when fibrosis was not developed. Several previous studies reported that MSCs administration did not improve pathologically established PF. Regarding the efficacy of IMRCs during the fibrosis phase, further studies are necessary and our investigation is ongoing. It is also noteworthy that some studies have raised concerns about MSCs potentially exacerbating pulmonary fibrosis [25], though the exact mechanisms underlying this phenomenon remain unclear. The ineffectiveness or potential adverse effects of

MSCs could stem from variations in fibrosis stage post-induction, species differences in model animals, and the timing of MSC administration relative to the inflammatory or fibrosis growth phases. Given that the cellular and molecular mechanisms specific to IPF-mediated effects of MSCs are not fully elucidated, clinical applications should proceed with caution.

The therapeutic mechanism of IMRCs in pulmonary fibrosis encompasses multiple facets, such as homing, paracrine signaling, immune modulation, and facilitation of tissue repair. In the previous study, IMRCs are unlikely to engraft or transdifferentiate into endothelial or epithelial cells after homing to the interstitium of lung tissues in vivo. Our scRNA-seq results also indicated that more than 99% of IMRCs expressed MMP1 compared with primary UCMSCs (< 1%). Given the role of MMP1 in degrading extracellular matrix, IMRCs may inhibit fibrosis by directly degrading deposited collagen through the secretion of MMP1. Additionally, IMRCs can secret a variety of anti-inflammatory factors that inhibit BLM-induced early inflammation, thereby further suppressing the progression of fibrosis. Notably, IMRCs exhibit a unique and high expression of the CD24 molecule, which acts as a crucial regulator of macrophage function. By modulating macrophage phenotype, IMRCs can inhibit inflammatory cascades, further contributing to their antifibrotic effects. However, the detailed mechanism of IMRCs in the treatment of pulmonary fibrosis has not been fully elucidated, and further studies are needed.

Conclusion

In summary, our findings show that IMRCs reduce lung inflammation and fibrosis in a route-dependent manner. Intravenous infusion of IMRCs has greater advantages compared with intratracheal infusion. Moreover, earlier and more frequent administrations of IMRCs is more beneficial to alleviate lung injury and pulmonary fibrosis. Furthermore, the mechanism for PF amelioration may be mediated to promote alveolar regeneration by paracrine actions and inhibit M1 type macrophages by CD24. This study is conducive to advancing the application of stem cells in the treatment of lung diseases.

Abbreviations

MSCs	Mesenchymal stem cells
IMRCs	immunity-and-matrix-regulatory cells
BLM	bleomycin
IPF	Idiopathic pulmonary fibrosis
hESCs	human embryonic stem cells
PF	pulmonary fibrosis
SARS-CoV-2	severe acute respiratory syndrome coronavirus 2
hEBs	human embryoid bodies
α-SMA	α-smooth muscle actin
FN	fibronectin
COL-I	collagen I
GFP	green fluorescence protein
IC	inspiratory capacity
Rrs	respiratory resistance
Crs	static compliance
Ers	elastic resistance
G	tissue damping
H	tissue elasticity
FVC	forced vital capacity
i.t.	Intratracheal
i.v.	Intravenous
BMSCs	bone marrow-derived MSCs
NIRF	Near-infrare fluorescence
Siglec-10	Sialic acid-binding Ig-like lectin 10
TLR	Toll-like receptor
EXO-CD24	CD24 positive exosomes
ARDS	Acute Respiratory Distress Syndrome

Supplementary Information

The online version contains supplementary material available at https://doi.org/10.1186/s13287-024-03945-4.

> Supplementary Material 1.
>
> Supplementary Material 2.

Author contributions

Dingyun Song, Zhongwen Li, Faguo Sun and Kaiwei Wu contributed equally to this original article. They completed majority of the experiments, wrote the manuscript with help from all the authors. They also designed the experiments, performed the data curation and drafted the entire article. Kan Zhang, Wenjing Liu, Kaidi Liu, Bin An, Zai Wang, Tiemei Zhao, Huaiyong Chen, Li Xiao, Liu Wang, Lixin Xie, Wei Li, Liang Peng participated in the experiments and data analysis. Huaping Dai, Jun Wu and Jie Hao contributed to the conception, design of the study, the data analysis, the revision of the manuscript, and the final approval of the version to be published. All authors contributed to the article and approved the final version of the manuscript.

Availability of data and materials

There are no datasets generated.

Declarations

Ethics approval and consent to participate

For animal experiments, the study entitled "Therapeutic effect of human embryonic stem cell derived mesenchymal stem cells on bleomycin induced pulmonary fibrosis in mice" was approved by the Experimental Animal Ethics Committee of China-Japan Friendship Hospital (Date: 27. 02. 2019, No.190108) and performed according to the Beijing Laboratory Animal Management Ordinance, guidelines. Our study involves IMRCs lines, therefore ethics approval is not applicable.

Consent for publication

Not applicable.

Competing interests

The authors declare that they have no competing interests.

Author details

[1]National Center for Respiratory Medicine; National Clinical Research Center for Respiratory Diseases; Institute of Respiratory Medicine, Chinese Academy of Medical Sciences; Department of Pulmonary and Critical Care Medicine, Center of Respiratory Medicine, China-Japan Friendship Hospital, Beijing 100029, China. [2]College of Pulmonary & Critical Care Medicine, 8th Medical Center of Chinese, PLA General Hospital, PLA General Hospital, Beijing 100091, China. [3]State Key Laboratory of Stem Cell and Reproductive Biology, Institute of Zoology, Chinese Academy of Sciences, Beijing 100101, China. [4]Key Laboratory of Organ Regeneration and Reconstruction, Chinese Academy of Sciences, Beijing 100101, China. [5]Beijing Institute for Stem Cell and Regenerative Medicine, Beijing 100101, China. [6]University of Chinese Academy of Sciences, Beijing 100049, China. [7]National Stem Cell Resource Center, Institute of Zoology, Chinese Academy of Sciences, Beijing 100101, China. [8]Institute of Clinical Medical Sciences, China-Japan Friendship Hospital, Beijing 100029, China. [9]Beijing Key Laboratory for Immune-Mediated Inflammatory Diseases, Institute of Medical Science, China-Japan Friendship Hospital, Beijing 100029, China. [10]Chinese Academy of Medical Sciences & Peking Union Medical College, Beijing 100730, China. [11]Tianjin Key Laboratory of Lung Regenerative Medicine, Haihe Hospital, Tianjin University, Tianjin 300350, China. [12]Key Research Laboratory for Infectious Disease Prevention for State Administration of Traditional Chinese Medicine, Tianjin Institute of Respiratory Diseases, Tianjin 300350, China. [13]Respiratory Research Institute, Senior Department of Pulmonary & Critical Care Medicine, the 8th Medical Center of PLA General Hospital, Beijing 100091, China.

References

1. Mura M. Use of nintedanib in interstitial lung disease other than idiopathic pulmonary fibrosis: much caution is warranted. Pulm Pharmacol Ther. 2020;66:101987.
2. Cruwys S, et al. Drug discovery and development in idiopathic pulmonary fibrosis: challenges and opportunities. Drug Discove Today. 2020;25(12):2277–83.
3. Phan THG, et al. Emerging cellular and molecular determinants of idiopathic pulmonary fibrosis. Cell and Mole Life Sci. 2021;78(5):2031–57. https://doi.org/10.1007/s00018-020-03693-7.
4. Wu J, et al. Immunity-and-matrix-regulatory cells derived from human embryonic stem cells safely and effectively treat mouse lung injury and fibrosis. Cell Res. 2020;30(9):1–16.
5. First case of COVID-19 infused with hESC derived immunity- and matrix-regulatory cells. Cell Proliferation, 2020
6. Wu J, et al. Phase 1 trial for treatment of COVID-19 patients with pulmonary fibrosis using hESC-IMRCs. Cell Prolif. 2020. https://doi.org/10.1111/cpr.12944.
7. Qi G, et al. Accreditation of biosafe clinical-grade human embryonic stem cells according to Chinese regulations. Stem Cell Reports. 2017;9:366–80.
8. Szapiel SV, et al. Bleomycin-induced interstitial pulmonary disease in the nude, athymic mouse. Am Rev Respir Dis. 1979;120(4):893.
9. Barkal AA, et al. CD24 signalling through macrophage Siglec-10 is a target for cancer immunotherapy. Nature. 2019;572(7769):392–6.
10. Wu J, et al. Immunity-and-matrix-regulatory cells derived from human embryonic stem cells safely and effectively treat mouse lung injury and fibrosis. Cell Res. 2020;30(9):794–809.
11. Zhu YG, et al. Adult stem cells for acute lung injury: remaining questions and concerns. Respirology. 2013;18(5):744–56.
12. Yan X, et al. Injured microenvironment directly guides the differentiation of engrafted Flk-1+ mesenchymal stem cell in lung. Exp Hematol. 2007;35(9):1466–75.
13. Curley GF, Hayes M, Ansari B, Shaw G, Ryan A, Barry F, O'Brien T, O'Toole D, Laffey JG. Mesenchymal stem cells enhance recovery and repair following ventilator-induced lung injury in the rat. Thorax. 2012;67(6):496–501. https://doi.org/10.1136/thoraxjnl-2011-201059.
14. Saito S, et al. Mesenchymal stem cells stably transduced with a dominant-negative inhibitor of CCL2 greatly attenuate bleomycin-induced lung damage. Am J Pathol. 2011;179(3):1088–94.
15. Sgalla G, et al. Idiopathic pulmonary fibrosis: pathogenesis and management. Respir Res. 2018;19(1):32.
16. Betensley A, Sharif R, Karamichos D. A systematic review of the role of dysfunctional wound healing in the pathogenesis and treatment of idiopathic pulmonary fibrosis. J Clin Med. 2017;6(1):2.
17. Ortiz LA, et al. Mesenchymal stem cell engraftment in lung is enhanced in response to bleomycin exposure and ameliorates its fibrotic effects. Proc Natl Acad Sci. 2003;100(14):8407–11.
18. Sun Z, et al. Inhibition of Wnt/β-Catenin signaling promotes engraftment of mesenchymal stem cells to repair lung injury. J Cell Phys. 2014;229:213.
19. Wang, et al., *Bone marrow mesenchymal stem cells attenuate silica-induced pulmonary fibrosis via paracrine mechanisms.* Toxicology Letters An International Journal Providing A Forum for Original & Pertinent Contributions in Toxicology Research, 2017
20. Shen Q, et al. Paracrine factors from mesenchymal stem cells attenuate epithelial injury and lung fibrosis. Mol Med Rep. 2015;11(4):2831.
21. Chen W, et al. Induction of siglec-G by RNA viruses inhibits the innate immune response by promoting RIG-I degradation. Cell. 2013;152(3):467–78.
22. Chen GY, et al. Amelioration of sepsis by inhibiting sialidase-mediated disruption of the CD24-SiglecG interaction. Nat Biotechnol. 2011;29(5):428.
23. Guo-Yun, et al., *CD24 and Siglec-10 Selectively Repress Tissue Damage-Induced Immune Responses.* Science, 2009
24. Kolb P, et al. The importance of interventional timing in the bleomycin model of pulmonary fibrosis. Eur Respir J. 2020;55(6):1901105.
25. Weiss DJ, Ortiz LA. Cell therapy trials for lung diseases: progress and cautions. Am J Respir Crit Care Med. 2013;188(2):123–5.

Publisher's Note